SAR/ISAR ADVANCED IMAGE RECONSTRUCTION ALGORITHMS

Andon Lazarov, Chavdar Minchev, Dimitar Minchev, Atanas Dimitrov
Burgas Free University

***Abstract**: In this work SAR/ISAR (Inverse Synthetic Aperture Radar/Inverse Synthetic Aperture Radar) parametric image reconstruction concepts are discussed. First, an image reconstruction procedure based on l_0 norm optimization is developed and applied over reduced number of measurements defined by randomly generated azimuth and range sensing matrices. Second, Kalman algorithm is applied for ISAR image extraction. Vector measurement and state equations are derived. Approximation functions based on LFM signal are defined. Results of numerical experiments are presented.*

***Key words**: SAR/ISAR*

1. Introduction

Synthetic Aperture Radar (SAR) and Inverse Synthetic Aperture Radar (ISAR) are advanced tools for monitoring the targets and relief of the earth's surface by probing with high informative electromagnetic pulses and registration of backscattered radiation [1-2]. The resulting images are depicted in a two-dimensional coordinate system defined by the slant range and azimuth (cross range) coordinates. High resolution on the slant range direction is realized by using wide bandwidth emitted pulses while high resolution on the cross range is achieved by coherent summation of reflected signals during the aperture synthesis, the time of observation.

Conventional nonparametric SAR/ISAR imaging algorithms are based on the spectral-correlation theory of the matched filter. The transmitted signal bandwidth and the synthetic aperture length limit their resolution capability. Compressed sensing (CS) and Kalman recurrent filtration are new approaches for the target imaging beyond the Nyquist sampling constraints. The former method is applied to solve the imaging problem using convex optimization. The latter method requires a recurrent minimum mean square definition of the problem to extract the image of the target. SAR imaging algorithms with a reduced number of collected samples by application of a CS method for along-track interferometric SAR is suggested in [3]. A SAR high resolution imaging method for sparse targets reconstruction based on l_1 norm minimization with only a small number of SAR echo samples is discussed in [4]. A data acquisition system for wideband SAR imaging and reconstruction of sparse signals from a small set of non-adaptive linear measurements based on CS by exploiting sparseness of point-like targets in the image space and by solving a convex l_1 minimization problem is presented in [5]. 3D imaging method for stepped frequency ground penetrating radar based on compressive sensing is suggested in [6]. A fast approach for overcomplete sparse decomposition based on l_0 smoothed norm and applications of compressed sensing for multiple transmitters multiple azimuth beams SAR imaging are presented in [7] and [8], respectively. Generating dense and super-resolution ISAR image by combining bandwidth extrapolation and compressive sensing is discussed in [9].

The main goal of this work is to suggest SAR/ISAR image reconstruction algorithms by applying compressed sensing technique and recurrent Kalman filtration. The rest of the paper is organized as follows. In Section 2 SAR/ISAR signal model is described. In Section 3, a sparse decomposition approach to solve the image reconstruction problem based on l_0 norm minimization is discussed. In Section 4, Kalman recurrent procedure is described. In Section 5, conclusions are made.

2. SAR/ISAR signal model

Assume the SAR/ISAR transmitter emits series of LFM electromagnetic pulses analytically described by the expression

$$S(t) = \sum_{p=1}^{M} \mathbf{rect}\frac{t - pT_p}{T} \mathbf{exp}\left[- j\left(\omega t + bt^2\right)\right] \tag{1}$$

where $\mathbf{rect}\dfrac{t - pT_p}{T} = \begin{cases} 1, \ 0 \le \dfrac{t - pT_p}{T} < 1 \\ 0, \mathbf{otherwise} \end{cases}$

where T_p is the pulse repetition period. $\omega = 2\pi\dfrac{c}{\lambda}$ is the angular frequency. $p = \overline{1,\ N}$ is the current number of the emitted LFM pulse. N is the total number of emitted pulses during aperture synthesis, c = 3.10^8 m/s is the speed of the light, $b = \dfrac{\pi\Delta F}{T_k}$ is the LFM index. ΔF is the bandwidth of the emitted pulse, and defines the range resolution, $\Delta R = c / 2\Delta F$. T is the time duration of LFM pulse.

The deterministic component of the SAR signal reflected from the *ij*-th point scatterer for particular *p* as a finite function can be written as

$$S_{mn}(t) = a_{ij} . \mathbf{rect}\frac{t - t_{ij}}{T} . \mathbf{exp}\left\{- j\left[\omega\left(t - t_{ij}\right) + b(t - t_{ij})^2\right]\right\} \tag{2}$$

where

$$\mathbf{rect}\frac{t - t_{ij}(p)}{T_k} = \begin{cases} 1, \dfrac{t - t_{ij}(p)}{T_k} \le 1, \\ 0, \mathbf{otherwise} \end{cases} \tag{3}$$

a_{ij} is the reflectivity coefficient of the *ij*-th point scatterer, $t_{ij}(p) = \dfrac{2R_{ij}(p)}{c}$ is the time delay of the signal from theb *ij*-th point scatterer. The deterministic component of the SAR/ISAR signal reflected from the entire surface can be regarded as a geometrical sum of the signals reflected by all point scatterers from the surface of observation and can be expressed as

$$S(t) = \sum_i \sum_j a_{ij} . \mathbf{rect}\frac{t - t_{ij}(p)}{T_k} . \mathbf{exp}\left\{- j\left[\omega\left(t - t_{ij}(p)\right) + b(t - t_{ij}(p))^2\right]\right\}, \tag{4}$$

where $t = t_{ij\,\min}(p) + (k-1)\Delta T$ is the fast time measured on the range direction. $k = \overline{0, K_{\max}(p)-1}$ is the range sample (fast time) index. ΔT is the timewidth of the LFM sample. $K_{\max}(p)$ is the number of the range bin where the SAR signal from the furthest point scatterer is detected, $t_{ij\,\min}(p) = \dfrac{2R_{ij\,\min}(p)}{c}$ is the time delay of the signal from the nearest point scatteter, $R_{ij\,\min}(p)$ is the distance to the nearest point scatteter on the surface of observation, calculated for the *p*-th emitted pulse.

Based on Taylor expansion of the exponential power $\omega\left(t - t_{ij}(p)\right) + b(t - t_{ij}(p))^2$ in the field of unknown discrete coordinates $\hat{p}$ and $\hat{k}$ of the *ij*-th point scatterers, (4) can be rewritten as

$$S(p,k) = \sum_{\hat{p},\hat{k}} a(\hat{p},\hat{k}).\exp\left\{-j\left[2.\pi.\frac{p.\hat{p}}{\hat{N}} + 2.\pi.\frac{k.\hat{k}}{\hat{K}} + \Phi(p,k)\right]\right\}, \quad (5)$$

where $a(\hat{p},\hat{k})$ is the image function, the projection of a_{ij} onto (*p*, *k*) signal plane, $\Phi(p,k)$ is the phase term of second and higher order, $\hat{p} = \overline{0, \hat{N}-1}$, $\hat{k} = \overline{0, \hat{K}-1}$, $\hat{N}$ and $\hat{K}$ denote the full number of reference image points on cross range direction and range direction, respectively.

3. Sparse decomposition approach to solve the image reconstruction problem

Assume $\Phi(p,k) = 0$, then (5) in matrix form can be rewritten as [10]

$$\mathbf{S} = \mathbf{P}.\mathbf{A}.\mathbf{K}^T \quad (6)$$

where $\mathbf{S}(N \times K)$ is the full length measurement signal matrix, $\mathbf{P}(N \times \hat{N}) = \left[\exp\left(-j\dfrac{2\pi p.\hat{p}}{\hat{N}}\right)\right]$ is the cross range Discrete Fourier Transform (DFT) matrix (cross-range matrix-dictionary), $\mathbf{K}(K \times \hat{K}) = \left[\exp\left(-j\dfrac{2\pi k.\hat{k}}{\hat{K}}\right)\right]$ is the range DFT matrix (range matrix-dictionary), $\mathbf{A}(\hat{N} \times \hat{K})$ is the image matrix.

Expression (6) denotes 2-D discrete Fourier decomposition of the sar signal in A matrix form. It means that the two-dimensional signal $\mathbf{S} \in \mathbf{R}^{N \times K}$ is a linear combination of columns of matrices P and K. In case $N = \hat{N}$ (complete measurement) the decomposition (6) is unique, it means that there exists a unique sparsest solution for A. Define compressed measurement matrix

$$\mathbf{X} = \mathbf{\Phi}_p.\mathbf{S}.\mathbf{\Phi}_k^T + \mathbf{W} \in \mathbf{R}^{N' \times K'}, \quad (7)$$

over the redundant Fourier dictionaries $\hat{\mathbf{P}} = \mathbf{\Phi}_p.\mathbf{P} \in \mathbf{R}^{N' \times \hat{N}}$ and $\hat{\mathbf{K}} = \mathbf{\Phi}_k \mathbf{K} \in \mathbf{R}^{K' \times \hat{K}}$, where $\mathbf{\Phi}_p(N' \times N)$ and $\mathbf{\Phi}_k(K' \times K)$ are pseudo identity sensing matrices, $\mathbf{W}$ is the white Gaussian noise matrix. In overcomplete case $N' < \hat{N}$ and $K' < \hat{K}$ the matrix $\mathbf{X}$ does not have unique decomposition. The image reconstruction problem can be solved by definition of sparse decomposition of the measurement signal as follows

$$\mathbf{min}\left\|\mathbf{A}\right\|_0 \text{ subject to } \left\|\mathbf{X} - \hat{\mathbf{P}}.\mathbf{A}.\hat{\mathbf{K}}^T\right\|_2^2 \le \varepsilon, \tag{8}$$

where $\mathbf{min}\left\|\mathbf{A}\right\|_0$ is the l_0- norm that denotes the number of non-zero point scatterer intensities in image matrix A, that means to find out the image matrix A with as much zero entries as possible, $\left\|\mathbf{X} - \hat{\mathbf{P}}.\mathbf{A}.\hat{\mathbf{K}}^T\right\|_2^2$ denotes the square of the Euclidian norm, ε is a small constant. A Gaussian function is used to approximate the l_0 - norm, i.e.

$$\left\|\mathbf{A}\right\|_0 = \hat{N}.\hat{K} - \sum_{\hat{p}=0}^{\hat{N}-1}\sum_{\hat{k}=0}^{\hat{K}-1} \mathbf{exp}\left(-\frac{\hat{a}_{\hat{p},\hat{k}}^2}{2\sigma^2}\right) \tag{9}$$

where σ is the variance of the white Gaussian noise. Then l_0-norm, $\mathbf{min}\left\|\mathbf{A}\right\|_0$ can be obtained be maximizing of the Gaussian function $F_\sigma(\mathbf{A}) = \sum_{\hat{p}=0}^{\hat{N}-1}\sum_{\hat{k}=0}^{\hat{K}-1} \exp\left(-\frac{\hat{a}_{\hat{p},\hat{k}}^2}{2\sigma^2}\right)$ onto the feasible set $\left\{\mathbf{A}\middle|\mathbf{X} = \hat{\mathbf{P}}.\mathbf{A}.\hat{\mathbf{K}}^T\right\}$ by a steepest ascent algorithm followed by projection onto the feasible set. Maximization of $F_\sigma(\mathbf{A})$ means increasing the number of zeros entries in the image matrix A.

4. Numerical experiment

SAR parameters: carrier frequency 10^{10} Hz, frequency bandwidth $\Delta F = 2.5.10^7$ Hz, pulse repetition period $2.5.10^{-3}$ s, LFM pulsewidth $2.5.10^{-6}$ s, number of emitted pulses $N_p = 1024$, number of range samples $K = 1024$. The geometry of the observed scene is defined by standard „peaks” function. The full length SAR signal reflected from the „peaks” surface, modeled by the matrix decomposition (6) of the signal matrix S(1024×1024) is presented in Fig. 1. The original image of the relief described by the function „peaks” and extracted from the SAR signal with dimensions [1024×1024] is depicted in Fig. 2.

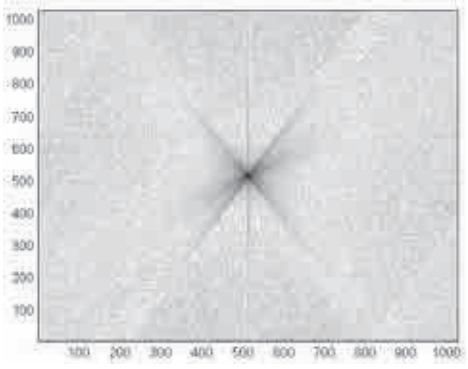

Fig. 1. SAR signal full length

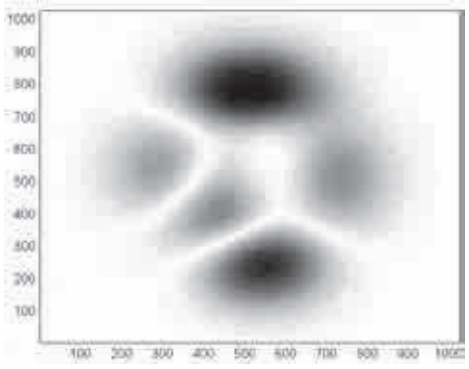

Fig. 2. Original image of the surface

Compressed sensing measurement matrix X(64×64) obtained by the multiplication of the signal complex matrix S(1024×1024) with sensing pseudo identity matrices $\mathbf{\Phi}_p(64\times1024)$ and $\mathbf{\Phi}_k(64\times1024)$, and additive Gaussian noise W(64×64) (Eq. 7), is presented in Fig. 3.

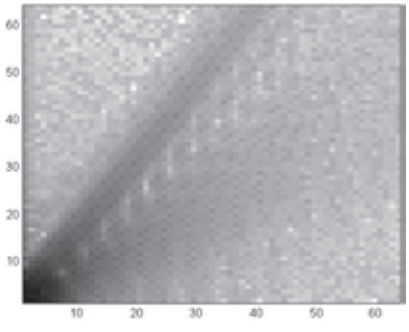

Fig. 3. Compressed sensing SAR signal

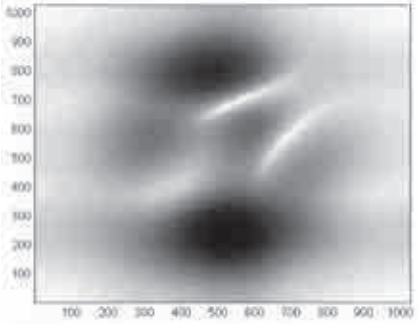

Fig. 4. SAR image obtained by l_0 norm

As can be seen in Fig. 4 the final image obtained from compressed sensing measurement data and reconstructed by application of l_0 norm optimization has satisfactory resolution. In comparison with the original image of the observed surface (Fig. 1), the main peaks of the observed surface are clearly defined in the image obtained by compressed sensing of measurement data (Fig. 4). The computational results prove the correctness of the signal model and image reconstruction algorithm based on sparse decomposition of the SAR signal and l_0 norm minimization.

5. Kalman Image Reconstruction

A. Vector Measurement Equation and State Equation

Kalman image reconstruction is a recurrent Kalman filtration defined by the following vector measurement and state equations

$$\begin{aligned}\boldsymbol{\xi}(p,k) &= \mathbf{S}\left[p,k,\mathbf{a}(p)\right]+\mathbf{n}(p,k)\\ \mathbf{a}(p) &= \mathbf{g}[p,k,\mathbf{a}(p-1)]+\mathbf{n}_0(p,k)\end{aligned} \tag{10}$$

where $\boldsymbol{\xi}(p,k)$ is the $[2(K+L);1]$ column vector, $\mathbf{S}[p,k,\mathbf{a}(p)]$ is the deterministic process in the field of vector arguments $\mathbf{a}(p)$, and yields a column-vector with dimensions $[2(K+L);1]$; $\mathbf{g}[p,k,\mathbf{a}(p-1)]$ is a column-vector function that describes the variation of the vector arguments at discrete time moments yielding dimensions of $[I\times J;1]$; $\mathbf{n}(p,k)$, $\mathbf{n}_0(p,k)$ are sequences of random vector values with zero expectation and covariance matrices $\psi(p,k)$ with dimensions $[2(K+L);2(K+L)]$ and $\mathbf{V}(p)$ with dimensions $[I\times J;I\times J]$, respectively. The vector $\mathbf{a}(p)$, with dimensions $[I\times J;1]$ accounts for a vector estimates of intensities of point scatterers $\dot{a}_{ij}$.

In order to model quadrature components of the ISAR trajectory signal, it is supposed that in the Cartesian coordinate space Oxy an object moves with a rectilinear trajectory at a constant speed $\mathbf{V}$. The object is situated in a coordinate grid whose origin may coincide with the geometric centre of the object. The shape of the object is described by the intensities (reflection coefficients) a_{ij} of point scatterers distributed in accordance with its geometry.

B. Approximation Functions

In the general case, the functions $\mathbf{S}[p,k,\mathbf{a}(p)]$ and $\mathbf{g}[p,k,\mathbf{a}(p-1)]$ in (10) would be non-linear. This circumstance would lead to ambiguity in invariant parameter definition. One of the main purposes of the present work is to reveal the composition of $\mathbf{S}[p,k,\mathbf{a}(p)]$ and $\mathbf{g}[p,k,\mathbf{a}(p-1)]$ under linear approximation and to develop an algorithm for a quasi-linear Kalman filtration of the invariant vector parameters in the complex amplitude of the ISAR trajectory signal.

The approximation function $\mathbf{S}[p,k,\mathbf{a}(p)]$ is defined by the quadrature components of a complex signal, reflected by the point scatterers, placed on the nods of a uniform grid, i.e.

$$\mathbf{S}[p,k,\mathbf{a}(p)]=\mathbf{S_c}[p,k,\mathbf{a}(p)]+j\mathbf{S_s}[p,k,\mathbf{a}(p)] \tag{11}$$

The Taylor's expansion after ignoring the higher order terms results in the following linear equations.

$$\mathbf{S_c}[p,k,\mathbf{a}(p)]=\mathbf{S_c}[p,k,\dot{\mathbf{a}}(p)]+\sum_{j=1}^{J}\sum_{i=1}^{I}\frac{\partial\mathbf{S_c}[p,k,\dot{\mathbf{a}}(p)]}{\partial a_{ij}}\left(a_{ij}-\dot{a}_{ij}\right) \tag{12}$$

$$\mathbf{S_s}[p,k,\mathbf{a}(p)]=\mathbf{S_s}[p,k,\dot{\mathbf{a}}(p)]+\sum_{j=1}^{J}\sum_{i=1}^{I}\frac{\partial\mathbf{S_s}[p,k,\dot{\mathbf{a}}(p)]}{\partial a_{ij}}\left(a_{ij}-\dot{a}_{ij}\right) \tag{13}$$

where $\dot{\mathbf{a}}(p)=\left[\dot{a}_{11}...\dot{a}_{1J},\dot{a}_{21}...\dot{a}_{ij}...a_{IJ}\right]^T$ is the vector-estimates of the invariant geometrical parameters with dimensions $[I\times J;1]$, the superscript „^{T}“ denotes matrix transpose, the

product $I \times J$ denotes the full number of estimates of isotropic point scatterers of the grid with intensity $\dot{a}_{ij}$. The constant coefficients of the Taylor expansion is defined by

$$\mathbf{S_c}\left[p,k,\dot{\mathbf{a}}(p)\right] = \sum_{j=1}^{J}\sum_{i=1}^{I}\dot{a}_{ij}\cos\left[\omega(t-t_{ij})+b(t-t_{ij})^2\right] \tag{14}$$

$$\mathbf{S_s}\left[p,k,\dot{\mathbf{a}}(p)\right] = \sum_{j=1}^{J}\sum_{i=1}^{I}\dot{a}_{ij}\sin\left[\omega(t-t_{ij})+b(t-t_{ij})^2\right] \tag{15}$$

The coefficients of the linear terms of the Taylor's expansion (12) defined by the expressions

$$\frac{\partial \mathbf{S_c}\left[p,k,\dot{\mathbf{a}}(p)\right]}{\partial a_{ij}} = \mathbf{cos}\left[\omega(t-t_{ij})+b(t-t_{ij})^2\right] \tag{16}$$

$$\frac{\partial \mathbf{S_s}\left[p,k,\dot{\mathbf{a}}(p)\right]}{\partial a_{ij}} = \mathbf{sin}\left[\omega(t-t_{ij})+b(t-t_{ij})^2\right]. \tag{17}$$

If the vector-estimated parameters are Gaussian and Markov, the state transition matrix function $\mathbf{g}\left[p,k,\mathbf{a}(p-1)\right]$, linking the vector estimates of invariant parameters in two consecutive moments in linear approximation, is given by the expression

$$\mathbf{g}\left[p,k,\mathbf{a}(p-1)\right] = \mathbf{g}(p,k).\dot{\mathbf{a}}(p-1) \tag{18}$$

where $\mathbf{g}(p,k) = \mathbf{diag}\left[\mathbf{exp}\left(\frac{NT_p}{\tau_{ij}}\right)\right]$ is the diagonal matrix with dimensions $\left[I \times J; I \times J\right]$, τ_{ij} is the correlation time of the parameter a_{ij} .

If the observation time, NT_p, is considerably less than the correlation time, τ_{ij}, then the state transition matrix $\mathbf{g}(p,k)$ becomes approximately an identity matrix, i.e., the estimated geometrical parameters are invariant in the ISAR observation time interval.

C. Recurrent Kalman Procedure

The modified recurrent Kalman procedure for quasilinear estimation of the invariant parameters can be defined as follows

$$\dot{\mathbf{a}}(p) = \mathbf{g}(p,k).\dot{\mathbf{a}}(p-1) + \mathbf{K}(p,k)\left\{\xi(p,k) - \mathbf{S}\left[p,k,\dot{\mathbf{a}}(p-1)\right]\right\} \tag{19}$$

where

$$\xi(p,k) = \left[\xi_{\mathbf{c}}(p,k),\ \xi_{\mathbf{s}}(p,k)\right]^T \tag{20}$$

is the new measurement vector with dimensions $\mathbf{[}2(K+L)\mathbf{;1]}$;

$$\mathbf{S}\left[p,k,\mathbf{a}(p-1)\right]=\begin{Bmatrix}\mathbf{S_c}\left[p,k,\mathbf{a}(p-1)\right]\\ \mathbf{S_s}\left[p,k,\mathbf{a}(p-1)\right]\end{Bmatrix} \tag{21}$$

is the measurement prediction vector with dimensions $\mathbf{[}2\mathbf{(}K+L\mathbf{);1]}$;

$$\mathbf{K}(p,k)=\mathbf{R}(p,k)\mathbf{H}^T(p,k)\psi^{-1}(p,k) \tag{22}$$

is the Kalman filter gain - matrix with dimensions $\mathbf{[}I\times J\mathbf{;}2\mathbf{(}K+L\mathbf{)]}$; $\mathbf{R}(p,k)$ is the update state error covariance matrix with dimensions $\left[I\times J\mathbf{;}I\times J\right]$, determined by

$$\mathbf{R}^{-1}(p,k)=\mathbf{H}^T(p,k)\psi^{-1}(p,k)\mathbf{H}(p,k)+\left[\mathbf{g}^T(p,k)\mathbf{R}(p-1,k)\mathbf{g}(p,k)+\mathbf{V}^{-1}(p,k)\right]^{-1} \tag{23}$$

Where

$$\mathbf{H}(p,k)=\begin{bmatrix}\frac{\partial\mathbf{S_c}\left[p,1,\dot{\mathbf{a}}(p-1)\right]}{\partial a_{11}}\mathbf{....}\frac{\partial\mathbf{S_c}\left[p,1,\dot{\mathbf{a}}(p-1)\right]}{\partial a_{IJ}}\\ \mathbf{.....}\qquad\mathbf{.....}\\ \frac{\partial\mathbf{S_c}\left[p,K,\dot{\mathbf{a}}(p-1)\right]}{\partial a_{11}}\mathbf{....}\frac{\partial\mathbf{S_c}\left[p,K,\dot{\mathbf{a}}(p-1)\right]}{\partial a_{IJ}}\\ \mathbf{.....}\qquad\mathbf{.....}\\ \frac{\partial\mathbf{S_s}\left[p,1,\dot{\mathbf{a}}(p-1)\right]}{\partial a_{11}}\mathbf{....}\frac{\partial\mathbf{S_s}\left[p,1,\dot{\mathbf{a}}(p-1)\right]}{\partial a_{IJ}}\\ \mathbf{.....}\qquad\mathbf{.....}\\ \frac{\partial\mathbf{S_s}\left[p,K,\dot{\mathbf{a}}(p-1)\right]}{\partial a_{11}}\mathbf{....}\frac{\partial\mathbf{S_s}\left[p,K,\dot{\mathbf{a}}(p-1)\right]}{\partial a_{IJ}}\end{bmatrix} \tag{24}$$

is the state-to-measurement transition matrix with dimensions $\left[2\mathbf{(}K+L\mathbf{);}I\times J\right]$.

The elements of the matrix $\mathbf{H}(p,k)$ for each $p=\overline{1,N}$ can be generally described by expressions:

$$h^c_{k,(i-1)J+j}=\frac{\partial\mathbf{S_c}\left[p,k,\dot{\mathbf{a}}(p-1)\right]}{\partial a_{ij}}=\mathbf{cos}\begin{bmatrix}\omega(t-t_{ij})+\\ +b(t-t_{ij})^2\end{bmatrix}, \tag{25}$$

$$h^s_{k,(i-1)J+j}=\frac{\partial\mathbf{S_s}\left[p,k,\dot{\mathbf{a}}(p-1)\right]}{\partial a_{ij}}=\mathbf{sin}\begin{bmatrix}\omega(t-t_{ij})+\\ +b(t-t_{ij})^2\end{bmatrix}. \tag{26}$$

The matrix $\mathbf{R}(p-1,k)$ is the predicted state error covariance matrix with dimensions $[I \times J; I \times J]$. In the beginning of the procedure $p=1$ the initial predicted state error covariance matrix $\mathbf{R}(0,k)$ is an identity matrix. The process noise covariance matrix $\mathbf{V}(p,k)$ and the measurement covariance matrix $\psi(p,k)$ are diagonal with elements $\frac{\mathbf{N}_0}{2T_p}$, where $\mathbf{N}_0$ is the spectral density of the Gaussian noise.

6. Numerical experiment

To substantiate the properties of the developed ISAR signal model and to verify the correctness of the developed Kalman image reconstruction procedure a numerical experiment is carried out. It is assumed that the target is moving rectilinearly in a 2-D observation Cartesian coordinate system Oxy and is detected in 2-D coordinate system $O'XY$. The trajectory parameters of the target are: the module of the vector velocity $V = 600$ m/s; the guiding angle of the vector velocity, $\alpha = \pi$; the angle between coordinate axes, $\varphi = 0$; the coordinates of the target geometric center at the moment $p = N/2$, i.e. the initial coordinates of the target geometric centre: $x_{00}(0) = 0$ m, $y_{00}(0) = 5.10^4$ m. The ISAR transmitted pulse is characterized be following parameters. The wavelength is $\lambda = 3.10^{-2}$ m. The pulse repetition period is $T_p = 2{,}5.10^{-2}$ s. The time duration of the transmitted LFM pulse is $T = 10^{-6}$ s. The number of samples of LFM ISAR signal is $K = 32$. The carry frequency is $f = 10^{10}$ Hz. The dimension of the LFM pulse discrete is $\Delta T = 3.125.10^{-8}$ s. The bandwidth of LFM transmitted signal is $\Delta F = 3.10^8$ Hz. The rate of linear frequency modulation is $b = 9{,}4.10^{14}$. The number of transmitted pulses during inverse aperture synthesis is $N = 100$. The target geometry is depicted in a 2-D regular rectangular grid, coordinate system $O'XY$ (Fig. 2). The dimensions of the grid's cell are $\Delta X = \Delta Y = 0{,}5$ m. The number of the reference points of the grid on the axes X is $I = 20$ and on the axis Y is $J = 20$ (Fig. 5). Point scatterers are placed at each node of the grid. The intensities of the point scatterers placed on the target are $a_{ij} = 0.01$. The intensities of the point scatterers placed out of the target are $a_{ij} = 0.001$. The arguments of approximation functions are intensities of point scatterers randomly distributed in the object space with amplitudes less than $\dot{a}_{ij} = 0.001$.

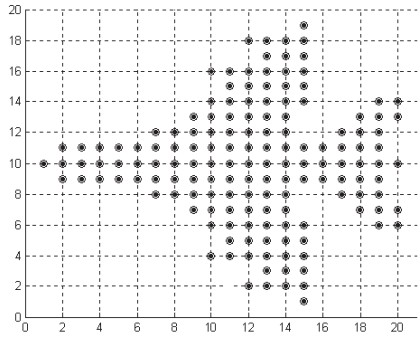

Fig.5. Discrete structure of the object depicted in the space of the regular grid

The results of the numerical experiment for different stages of the recurrent Kalman procedure are presented in Figs. 6-9.

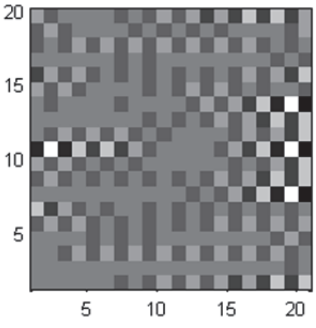

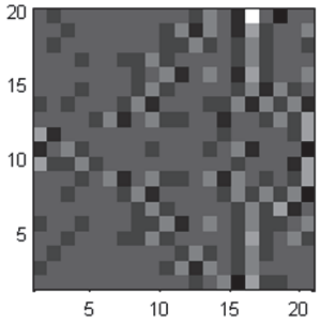

Fig. 6. ISAR image by p=1 step Fig 7. ISAR image by p=25 step

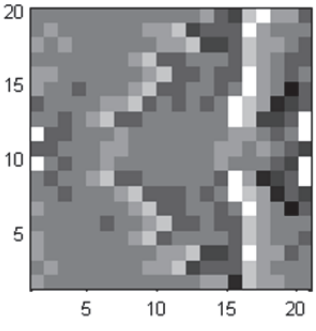

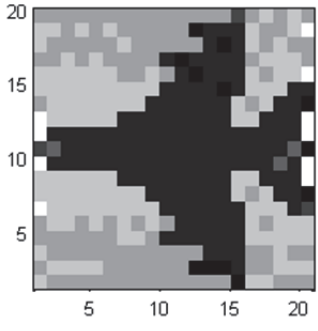

Fig 8. ISAR image by p=40 step Fig 9. ISAR image by p=100 step

As can be seen the quality of the ISAR images is improved with each iteration step. It proves the correctness of the ISAR signal model and image reconstruction capability of the Kalman method. The described Kalman algorithn distinguishes with high calculation speed, steady and quick convergence of computations. Therefore, it could be successfully exploited for extracting geometrical parameters from the LFM ISAR data.

7. Conclusions

First, a SAR image reconstruction algorithm based sparse decomposition has been developed. A model of LFM SAR signal reflected from the observed scene, a relief of the earth surface, has been presented as a matrix multiplication of three matrices: azimuth (cross range) inverse discrete Fourier transform (IDFT) matrix, image matrix and range IDFT matrix. Image reconstruction procedure based on l_0 norm optimization has been developed and applied over reduced number of measurements defined by randomly generated azimuth and range sensing matrices. The geometry of the scene has been described by standard „peaks” function. Results of numerical experiments has provided correctness of the developed algorithm.

Second, Kalman image reconstruction algorithm has been developed. Vector measurement and vector state equations have been defined. Based on LFM ISAR signal model approximation function have been derived. Recurrent Kalman procedure for quasilinear estimation of the geoemtrical parameters has been described. Simulation experiments have been carried out. It illustrates the capability of the recurrent method for ISAR imaging. The recurrent Kalman procedure demonstrates high effectiveness in the target image reconstruction using simulated ISAR data.

References

1. Nicolas, J-M, G. Vasile, M. Gay, Fl. Tupin, and Em. Trouvé. SAR processing in the temporal domain: application to direct interferogram generation and mountain glacier monitoring Can. J. Remote Sensing, Vol. 33, No. 1, 2007, pp. 52–59.
2. Van Leijen, F. R. Hanssen. Interferometric radar meteorology: resolving the acquisition ambiguity. In CEOS SAR Workshop, Ulm Germany, 27-28 May 2004, page 6, 2004.
3. Y.G. Lin, B.C. Zhang, W. Hong, Y.R. Wu. Along-track interferometric SAR imaging based on distributed compressed sensing, Electronics Letters, Vol. 46, No 12, 10 June 2010, p. 858 – 860.
4. S.-J. Wei, X.-L. Zhang, J. Shi, and G. Xiang, „Sparse reconstruction for SAR imaging based on compressed sensing,“ Progress in Electromagnetics Research, Vol. 109, 2010, pp. 63-81,
5. Ali C. Gurbuza, James H. McClellanb, Waymond R. Scott Jr.b. Compressive sensing for subsurface imaging using ground penetrating radar, Signal Processing, Volume 89, Issue 10, October 2009, pp. 1959–1972.
6. J.-L. Cai, C.-M. Tong, W.-J. Zhong, and W.-J. Ji, „3D imaging method for stepped frequency ground penetrating radar based on compressive sensing“, Progress In Electromagnetics Research M, Vol. 23, 2012, pp. 153-165.
7. H. Mohimani, M. Babaie-Zadeh, and C. Jutten, „A fast approach for overcomplete sparse decomposition based on smoothed norm,” IEEE Trans. on Signal Proc, vol. 57, no. 1, , January 2009, pp. 289–301.
8. J. Li, S. Zhang, and J. Chang, „Applications of compressed sensing for multiple transmitters multiple azimuth beams SAR imaging,“ Progress in Electromagnetics Research, Vol. 127, 2012, pp. 259-275.
9. Quan Y H, Zhang L, Guo R, et al. Generating dense and super-resolution ISAR image by combining bandwidth extrapolation and compressive sensing. Sci China Inf Sci, 2011, 54: pp. 2158–2169, doi: 10.1007/s11432011-4298-4
10. A. Ghaffari, M. Babaie-Zadeh, C. Jutter, and H. Moghaddam, „Sparse decomposition of two-dimensional signals”, Proceedings of IEEE International Conference on Acoustics, Speech and Signal Processing, 2009, pp. 3157-3160.